Electronic Supplementary Material (ESI) for New Journal of Chemistry.

Supporting Information

FRET based ratiometric switch for selective sensing of Al^{3+} with bio-imaging in human peripheral blood mononuclear cells PBMCs

Sangita Das[a*], Partha Pratim Das[b] , James W.Walton[a], Kakali Ghoshal[c], Lakshman Patra[d] and Maitree Bhattacharyya[c]

[a] *Durham University, Department of Chemistry, Durham, DH1 3LE, UK; Email: sangita.das@durham.ac.uk*

[b] *Department of Earth System Sciences, Yonsei University, Seoul 120749, Korea.*

[c] *Department of Biochemistry, University of Calcutta, 35 Ballygunge Circular Road, Kolkata 700019, India*

[d] *Department of Chemistry, Jadavpur University, Jadavpur, Kolkata, India*

CONTENTS

1. UV/vis Study

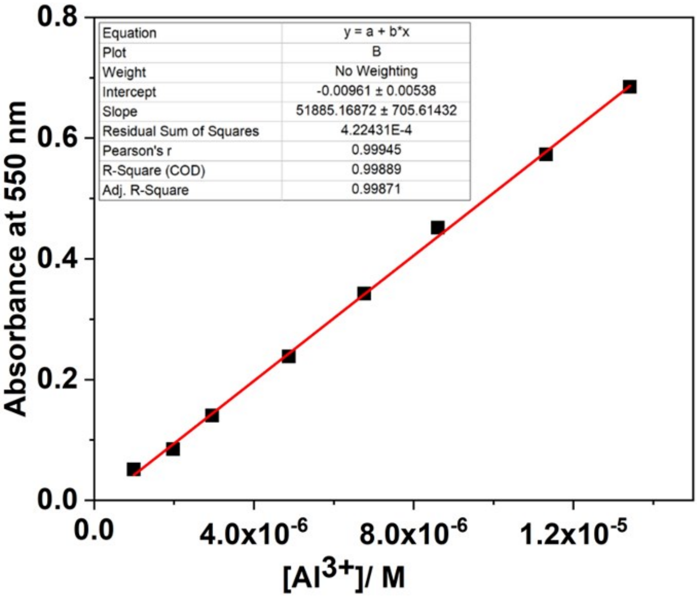

Equation	y = a + b*x
Plot	B
Weight	No Weighting
Intercept	-0.00961 ± 0.00538
Slope	51885.16872 ± 705.61432
Residual Sum of Squares	4.22431E-4
Pearson's r	0.99945
R-Square (COD)	0.99889
Adj. R-Square	0.99871

Determination of Limit of Detection

Figure S1: Absorbance intensity at 550 nm of TPRH depending on the concentration of Al^{3+}

The limit of detection (LOD) of TPRH towards Al^{3+} was determined from the following equation: LOD = K × Sb_1/S, where K = 3; Sb_1 is the standard deviation of the blank solution; S is the slope of the calibration curve.[1] From the data we find slope = 51900, and Sb_1 value is 0.0006. The calculated Limit of Detection was calculated as 3.5×10^{-8} M.

Determination of binding constant

The association constant was calculated, according to the Benesi-Hildebrand equation[2]:

$$1/(A-A_o) = 1/\{K(A_{max}-A_o)\ [M^{x+}]^n\} + 1/[A_{max}-A_o]$$

Here A_o and A are the absorbance of the probe at 550 nm in the absence of guest and in the presence of added guest, A_{max} is absorbance in presence of added $[M^{x+}]_{max}$ and K_a is the association constant calculated for Al^{3+} binding. The association constant (K_a) was determined from the slope of the straight line of the plot of $1/(A-A_o)$ against $1/[Al^{3+}]$. The association constant for TPRH was found to be 5.9×10^5 M^{-1}.

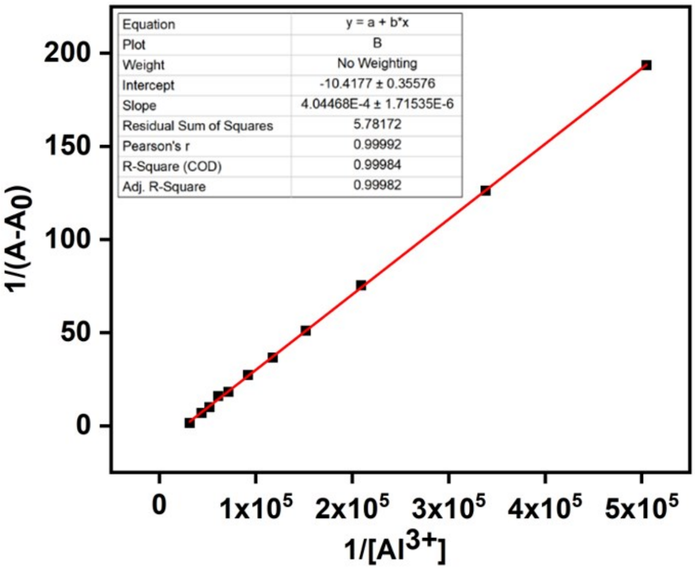

Figure S2: Benesi–Hildebrand plot from UV-Vis titration data of receptor (TPRH, 20 µM) with Al^{3+}.

2. Fluorescence Study

Determination of fluorescence Quantum Yield (Φ) of TPRH and its complex with Al^{3+}

To measure the quantum yields of TPRH and its complex with Al^{3+}, the absorbance of the compounds in methanol solution were recorded. The emission spectra were then recorded using the maximum excitation wavelengths, and the integrated areas of the fluorescence-corrected spectra were measured. The quantum yield of TPRH was then calculated by comparison with fluorescein (Φs = 0.97 in basic ethanol) as a reference. The quantum yield of TPRH-Al^{3+} was calculated by comparison with rhodamine B (Φs = 0.66 in ethanol) as a reference. In each case the following equation was used:

$$\Phi_x = \Phi_s \times \left(\frac{Ix}{Is}\right) \times \left(\frac{As}{Ax}\right) \times \left(\frac{nx}{ns}\right)^2$$

where, x and s indicate the unknown and standard solution, respectively, Φ is the quantum yield, I is the integrated area under the fluorescence spectra, A is the absorbance and n is the refractive index of the solvent. The quantum yield calculated for TPRH using the above equation was 0.21. The quantum yield calculated for TPRH-Al^{3+} using the above equation was 0.36.

Linear responsive curve of TPRH

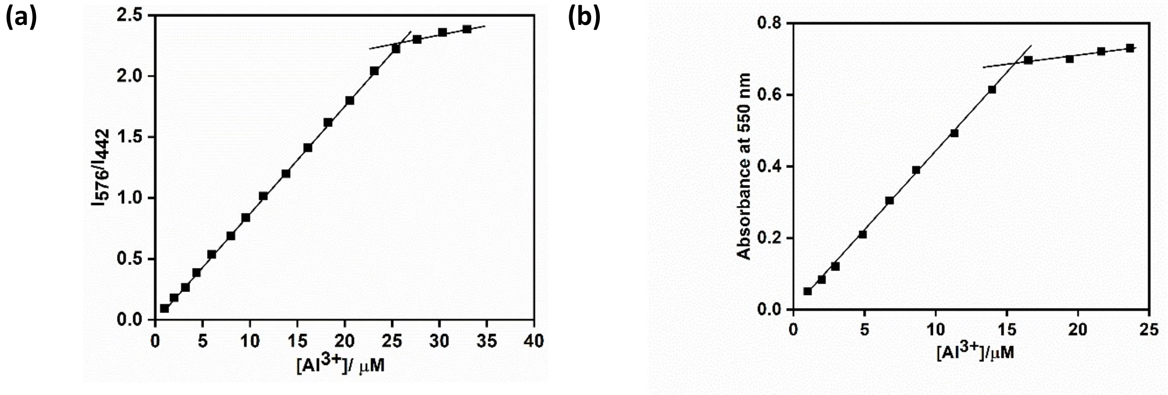

Figure S3: The response curve of (a) emission intensity ratio at I_{576}/I_{442} (in nm) and (b) absorbance at 550 nm of **TPRH** depending on the Al^{3+} concentration.

Limit of detection determination

The detection limit was calculated based on the fluorescence titration. To determine the S/N ratio, the emission intensity of **TPRH** without Al^{3+} was measured 10 times and the average and standard deviation of blank measurements was determined. The limit of detection (LOD) of TPRH towards Al^{3+} was determined from the following equation: LOD = K × Sb_1/S, where K = 3; Sb_1 is the standard deviation of the blank solution; S is the slope of the calibration curve.[1] For Al^{3+}:

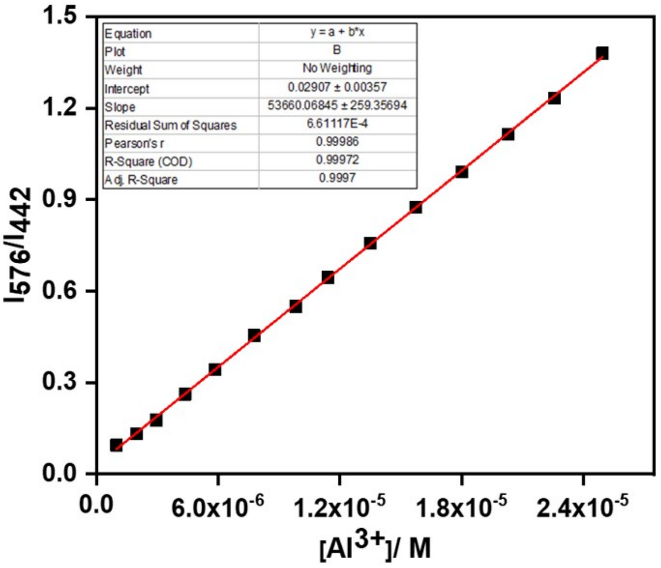

Figure S4: Emission intensity ratio I_{576}/I_{442} of TPRH depending on the concentration of Al^{3+}

From the data we find slope = 53700, and Sb_1 value is 0.0012. Thus, using the formula above the limit of detection is calculated as 6.7×10^{-8} M for TPRH.

Job Plot

Stock solution of TPRH and Al^{3+} were prepared at 2.0 x 10^{-5} M in buffered CH_3CN-H_2O (1:1, *v/v*). The emission at 576 nm was monitored as the molar ratio was varied, but equal total molar quantities maintained. A Job plot was drawn by plotting $\Delta I.X_{TPRH}$ *vs* X_{Al} (ΔI = change of intensity of the emission spectrum during titration and X_{TPRH} is the mole fraction of TPRH).

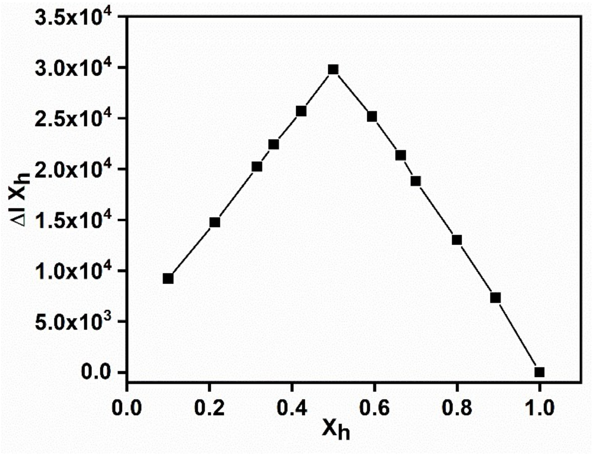

Figure S5: Job plot diagram of TPRH with Al^{3+} (where X_h is the mole fraction of TPRH and ΔI indicates the change of emission at 576 nm).

3. Calculation of FRET efficiency

FRET efficiency (E) of the probe (TPRH) was evaluated according to the following equation:

$$E = 1 - \frac{\Phi_D}{\Phi_D^0}$$

Where, Φ_D and $\Phi_D{}^0$ are the fluorescence quantum yields of the triphenylamine donor in the presence and absence of the rhodamine acceptor, respectively. Φ_D was obtained by fluorescence measurement of TPRH in the presence of 1 equivalents of Al^{3+} (TPRH-Al^{3+}), and $\Phi_D{}^0$ was obtained using the corresponding triphenylamine conjugated derivative (compound **1**). Quantum yields of both triphenylamine conjugated derivative (compound **1**) and TPRH-Al^{3+} were measured in methanol solution using fluorescein (Φ = 0.97 in basic ethanol) as standard. Both the donor and the TPRH-Al^{3+} were taken in 10 μM concentration. The FRET efficiency of TPRH was calculated to be 44%.

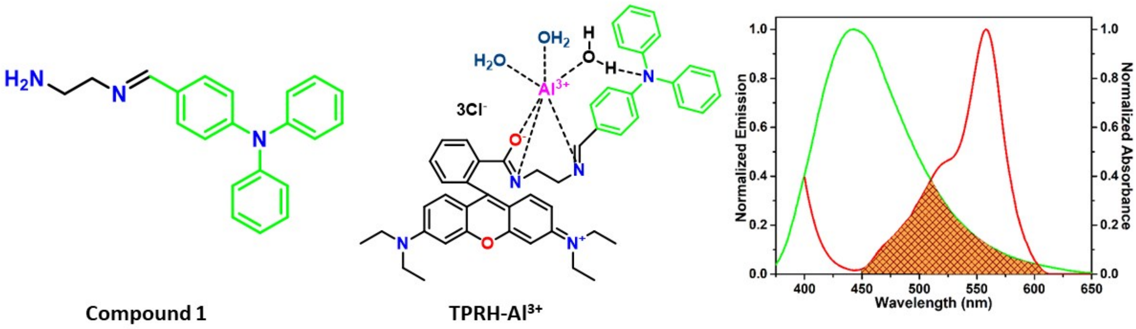

Compound 1

TPRH-Al^{3+}

Figure S6: The spectral overlap of donor emission (green line) and acceptor absorbance (red line) of TPRH. Here, the donor is compound **1** and the acceptor is TPRH-Al^{3+}. Spectra were recorded in MeOH/H_2O (1/4, v/v, pH = 7.2, 10 mM HEPES buffer solution), λ_{ex} = 350 nm.

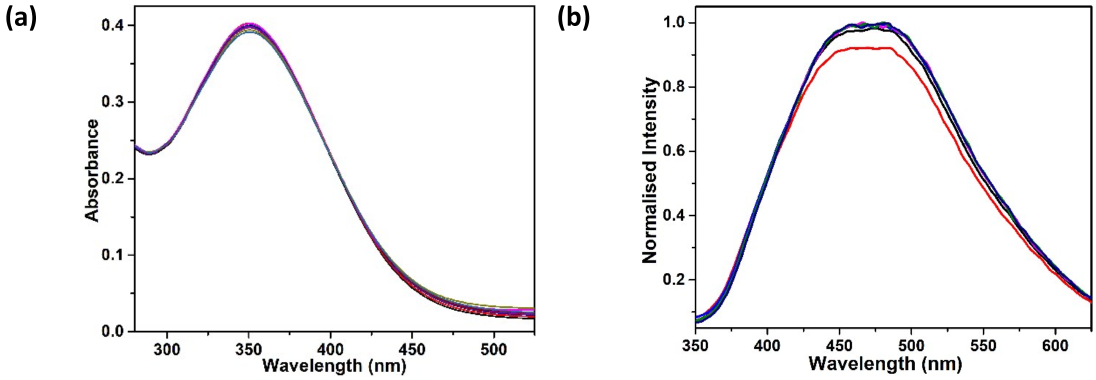

Figure S7: Change of (a) UV-vis and (b) emission spectra of compound 1 upon gradual addition of Al^{3+} (0 to 1.5 equivalents) (λex = 340 nm.).

Analogue of the rhodamine half of the molecule has already been reported by A. Lobnik *et.al* in Sensors 2018, 18, 1201; doi:10.3390/s18041201, and the probe is not sensitive towards Al^{3+}, which showed that the response is more than just the sum of the responses of each of the component halves.

4. Truth table for INHIBIT Logic Gate

Table S1

Input 1 (Al^{3+})	Input 2 (EDTA)	Output (Emission intensity at 442 nm)	Output (Emission intensity at 576 nm)
0	0	1	0
1	0	0	1
0	1	1	0
1	1	1	0

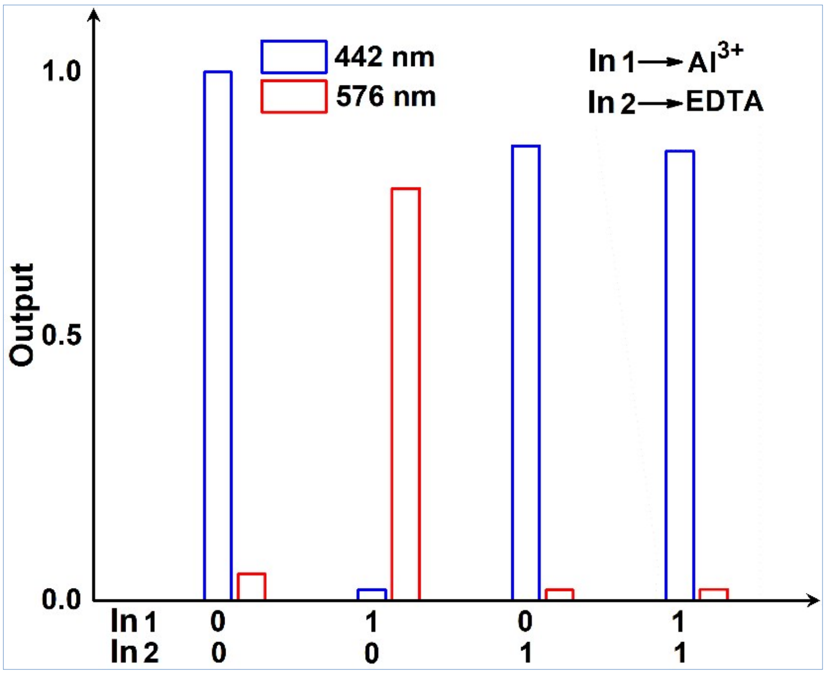

Figure S8: Combinatorial logic scheme of INHIBIT logic operations.

5. ^{1}H NMR spectrum of Compound 1

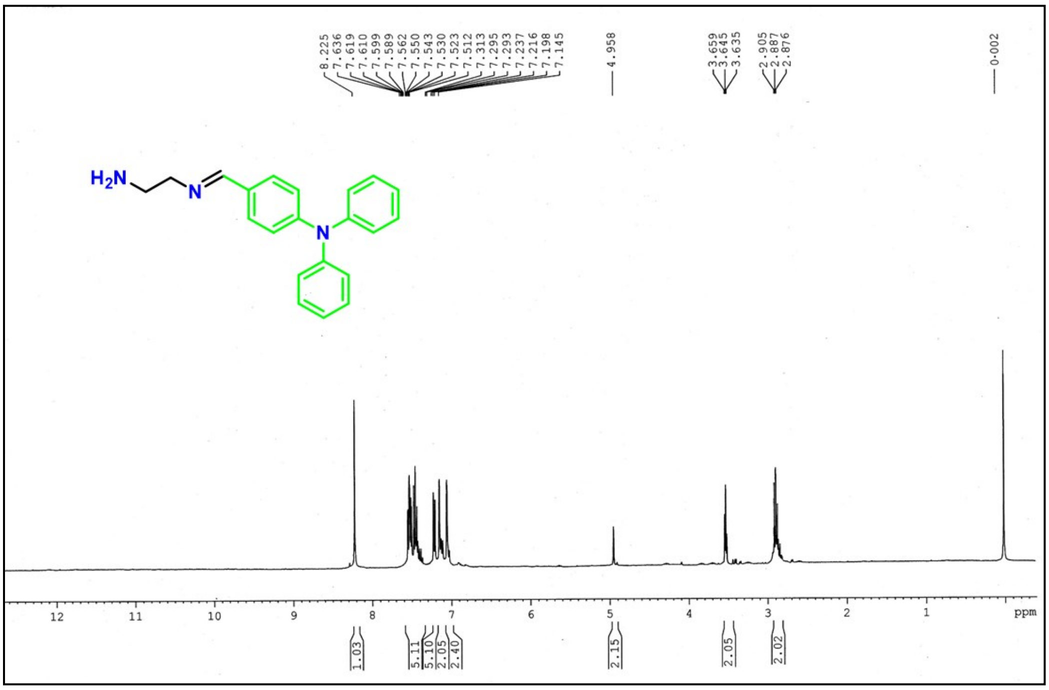

Figure S9: ^{1}H NMR (400 MHz) spectrum of Compound 1 in $CDCl_3$ (298 K).

6. ^{13}C NMR spectrum of Compound 1

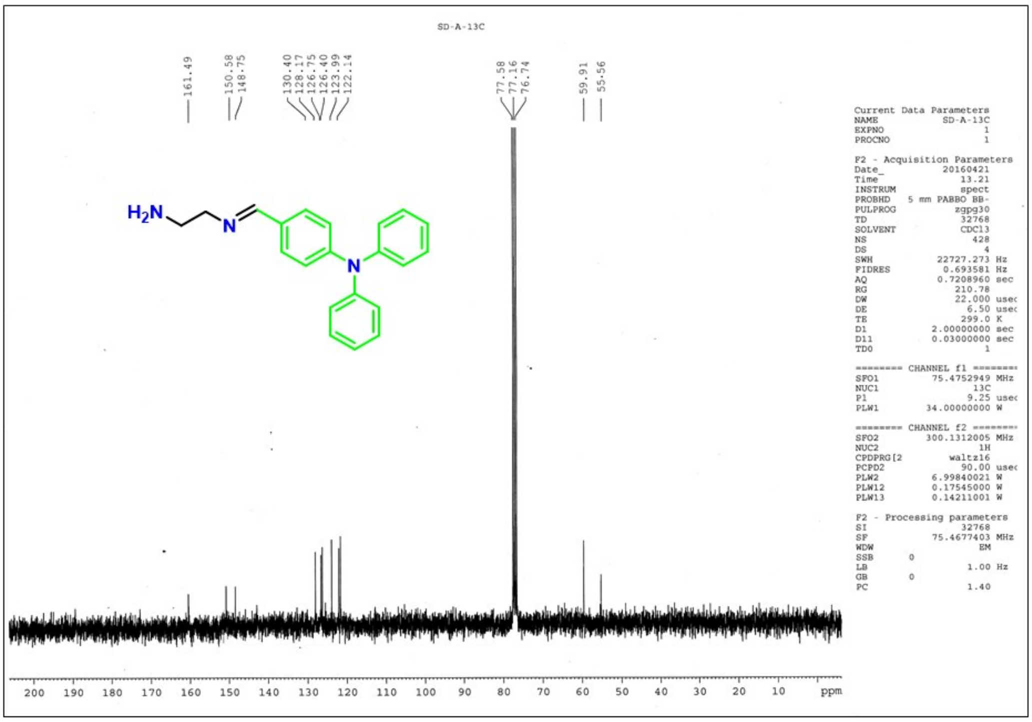

```
Current Data Parameters
NAME             SD-A-13C
EXPNO                   1
PROCNO                  1

F2 - Acquisition Parameters
Date_            20160421
Time                13.21
INSTRUM             spect
PROBHD   5 mm PABBO BB-
PULPROG           zgpg30
TD                 32768
SOLVENT            CDCl3
NS                   428
DS                     4
SWH            22727.273 Hz
FIDRES          0.693581 Hz
AQ             0.7208960 sec
RG                210.78
DW                22.000 usec
DE                  6.50 usec
TE                 299.0 K
D1            2.00000000 sec
D11           0.03000000 sec
TD0                    1

======== CHANNEL f1 ========
SFO1          75.4752949 MHz
NUC1                 13C
P1                  9.25 usec
PLW1         34.00000000 W

======== CHANNEL f2 ========
SFO2         300.1312005 MHz
NUC2                  1H
CPDPRG[2         waltz16
PCPD2              90.00 usec
PLW2          6.99840021 W
PLW12         0.17545000 W
PLW13         0.14211001 W

F2 - Processing parameters
SI                 32768
SF            75.4677403 MHz
WDW                   EM
SSB      0
LB                  1.00 Hz
GB       0
PC                  1.40
```

Figure S10: ^{13}C NMR (75 MHz) spectrum of Compound 1 in $CDCl_3$ (298 K).

7. Mass Spectrum of Compound 1

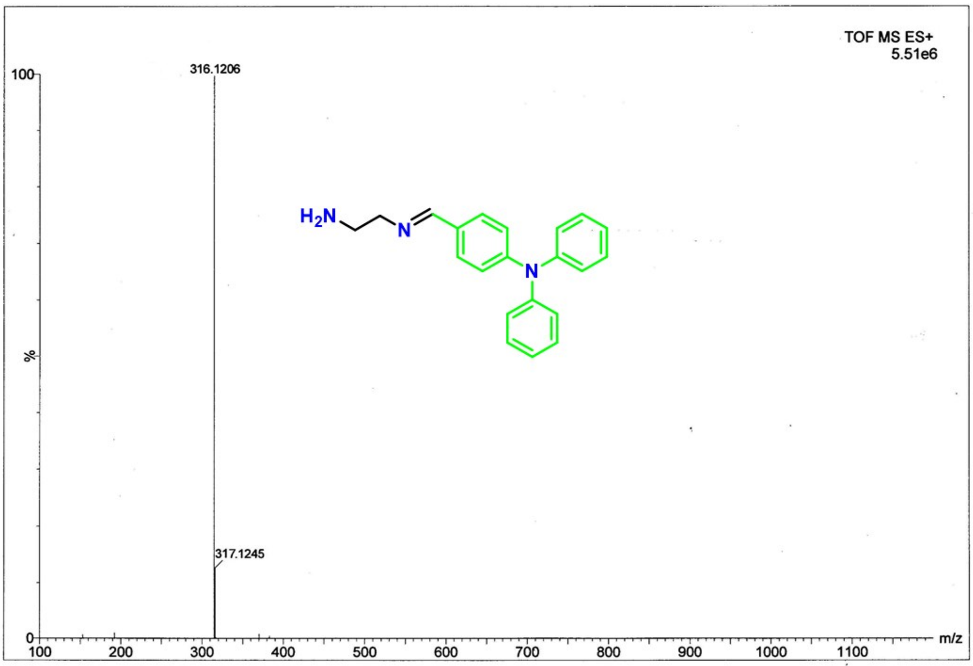

Figure S11: MS of Compound **1** (positive ESI mode). m/z 316.12; calcd for $C_{21}H_{22}N_3$ $[M+H]^+$ 316.18.

8. ^{1}H NMR spectrum of TPRH

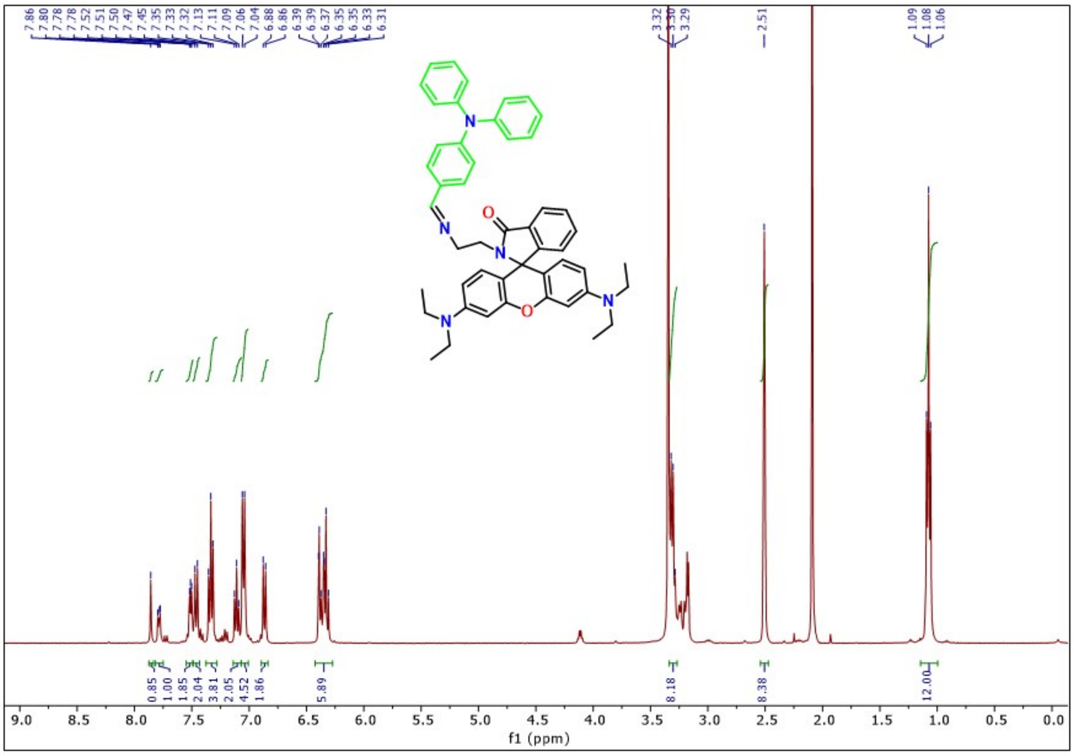

Figure S12: ^{1}H NMR (400 MHz) spectrum of TPRH in d_6-DMSO (298 K)

9. ^{13}C MR spectrum of TPRH

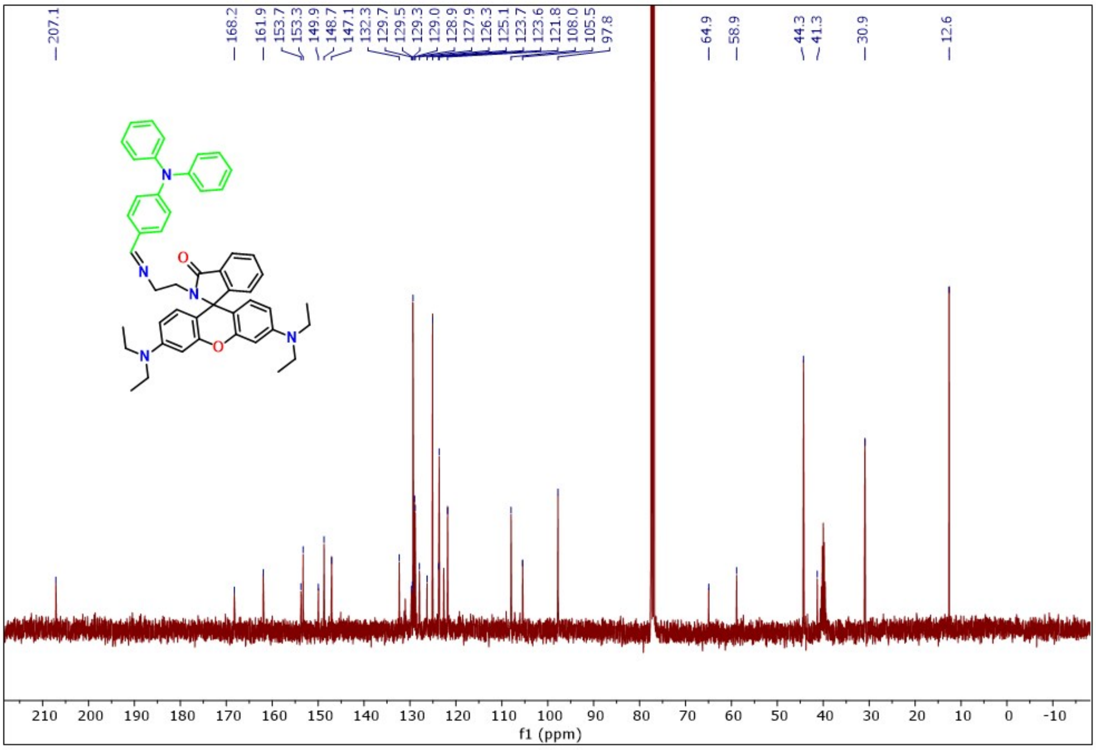

Figure S13: ^{13}C NMR (100 MHz) spectrum of TPRH in $CDCl_3$ (298 K).

10. Mass spectrum of TPRH

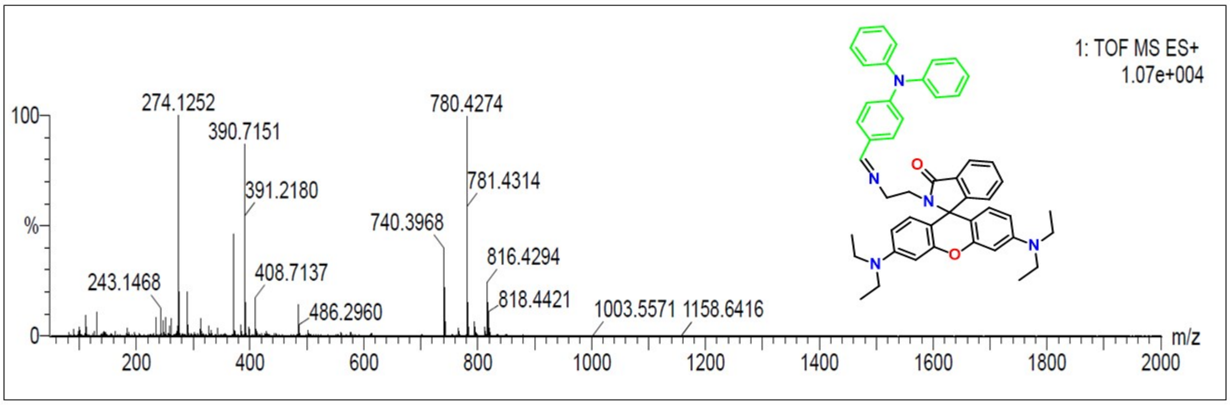

Figure S14: HRMS of TPRH (positive ESI mode). HRMS (ESI, positive mode): (m/z) found: 740.3968; calcd for $C_{49}H_{49}N_5O_2$ $[M+H]^+$ 740.3959.

11. Mass spectrum of the complex TPRH: Al^{3+}

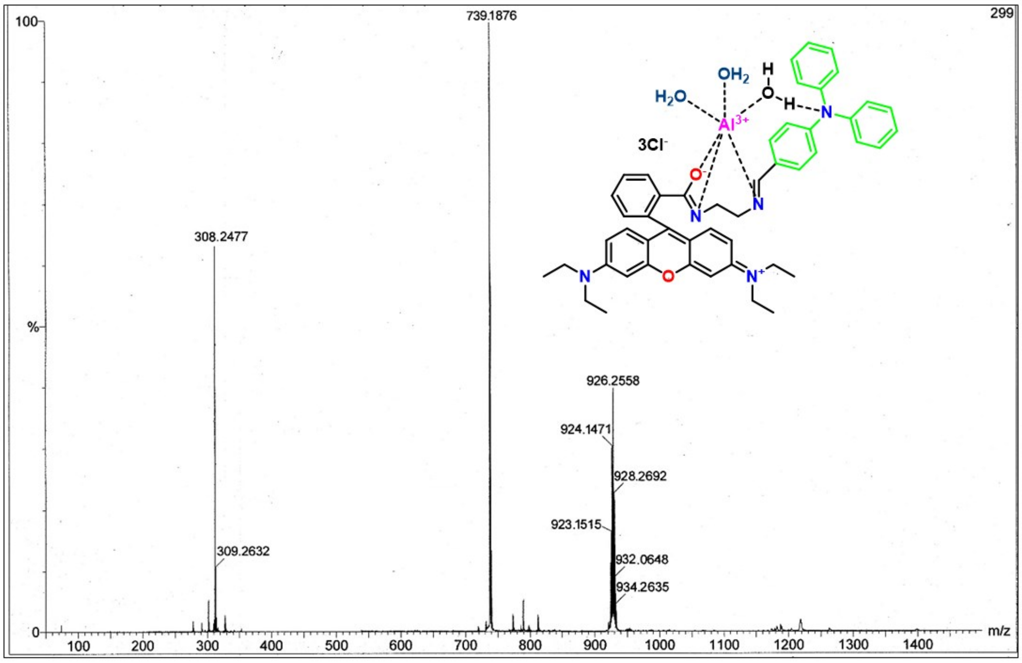

Figure S15: MS spectrum of the TPRH with Al^{3+} (positive ESI mode). *m*/*z* 926.26, $[TPRH + Al^{3+} + 3H_2O + 3^{35}Cl^- + H^+]^+$ requires 926.31.

12. ^{1}H NMR of TPRH and TPRH-Al^{3+}

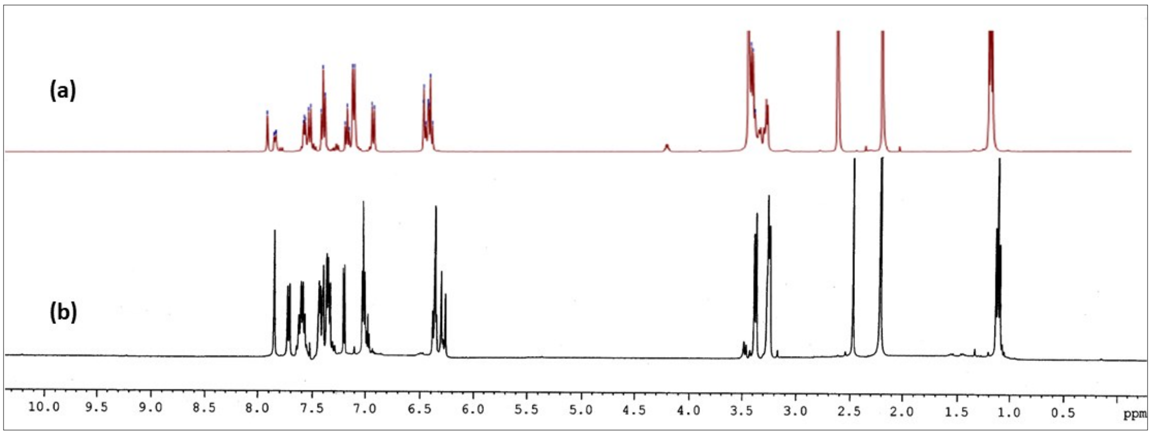

Figure S16: Partial ^{1}H NMR (400 MHz) spectra of (a) TPRH and (b) TPRH + Al^{3+} in d_6-DMSO. [TPRH] = 3.12×10^{-3} M; [Al^{3+}] = 6.24×10^{-3} M (298 K).

13. Comparison Table

Table S2

Sr. No	Fluorophore Used	Ratiometric Fluorescence Change	Detection Limit	Bioimaging Studies	Selective towards	Mechanism	Reference
1.	Rhodamine–naphthalene	Yes	8.06×10^{-8} M	No	Al^{3+}	FRET	Tetrahedron Letters 2016, 57, 1935–1939
2.	Rhodamine-linked pyridyl thiourea	Yes	1.08×10^{-4} M and 1.27×10^{-6} M for F^- and Al^{3+} ions respectively	Yes	F^-, Al^{3+} and Ag^+	FRET	Supramolecular Chemistry, 2015, 27, , 490–500
3.	Rhodamine-diformyl p-cresol	Yes	5×10^{-9} M	Yes	Al^{3+}	PET−CHEF and FRET	Inorg. Chem. 2013, 52, 3627−3633
4.	N-salicylidenehydrazide ligands- furan-	No	3.1×10^{-9} M	No	Al^{3+} and Zn^{2+}	Chelation-enhanced fluorescence (CHEF)	ACS Sens. 2016, 1, 144−150
5.	Antipyrine Schiff bases	No	4.97×10^{-7} M 9.60×10^{-7}	No	Al^{3+} and Cr^{3+}	PET	Sensors and Actuators B,

			M Respectively Al^{3+} and Cr^{3+}				2016, 231, 847–859
6.	2,5-diarylthiazolo[5,4-d]thiazole	No	Not given	No	Cr^{3+} and Al^{3+}	Off-On mechanism	Dyes and Pigments 2012, 94, 423-426
7.	Naphthaldehyde semicarbazone	No	6.75 ×10^{-8} M (Al^{3+})and 7.89×10^{-7} M (F^{-})	Yes	Cascade sensing of Al^{3+} and F^{-}	CHEF	RSC Adv., 2020, 10, 21629–21635
8.	Benzothiazol–furan	No	6.47 nM	Yes	Al^{3+}	PET and ESIPT	New J. Chem., 2020, 44, 12079-12089
9.	Anthracene-pyridinecarboxaldehyde	No	(4.338 ± 0.00032) x 10^{-11} (Al^{3+}) (5.865± 0.00011)) x 10^{-11} (Al^{3+})	No	Cr^{3+} and Al^{3+}	CHEF	New J. Chem., 2020,44, 12692-12703
10	Antipyrine	No	1.05 nM for Al^{3+}, 2.35 nM for Zn^{2+}	No	Al^{3+} and Zn^{2+}	Aggregation induced emission enhancement (AIEE)	Photochem. Photobiol. Sci., 2020,19, 681-694
11	Rhodamine-thiophene	No	4.17 × 10^{-6} M	No	Al^{3+}	Off-On mechanism	Luminescence 2016; 31, 851–855
12	Rhodamine-aminophenol	No	0.16 µM	Yes	Al^{3+}	Off-On mechanism	RSC Adv., 2018, 8, 31106–31112
13	Thiophene-based rhodamine	No	Fe^{3+} and Al^{3+} 5 and 6 µM, respectively	Yes	Fe(III) and Al^{3+}	Off-On mechanism	10.1007/s00216-017-0490-8
14	Naphthalimide	Yes	2.9 × 10^{-7} M	Yes	Al^{3+}	Intramolecular charge transfer (ICT)	New J. Chem., 2020,44, 3261-3267
15	Triphenylamine and rhodamine-B	Yes	6.7 × 10-8 M	Yes	Al^{3+}	FRET	Present Work

14. References

1. (a) M. Shortreed, R. Kopelman, M. Kuhn and B. Hoyland, *Anal. Chem.*, 1996, **68**, 1414; (b) W. Lin, L. Yuan, Z. Cao, Y. Feng and L. Long, *Chem. Eur. J.*, 2009, **15**, 5096.
2. (a) H. A. Benesi and J. H. Hildebrand, *J. Am. Chem. Soc.*, 1949, **71**, 2703; (b) D. C. Carter and J. X. Ho, *Adv. Protein Chem.*,1994, **45**, 153; (c) A. Mallick and N. Chattopadhyay, *Photochem. Photobiol.*, 2005, **81**, 419; (d) I. Ravikumar, B. N. Ahamed and P. Ghosh, *Tetrahedron*, 2007, **63**, 12940.